

# SENSITIVITY OF FUTURE $e^+e^-$ COLLIDERS TO PROCESSES OF DARK MATTER PRODUCTION WITH LIGHT MEDIATOR EXCHANGE\*

JAN KALINOWSKI, KRZYSZTOF MEKAŁA, PAWEŁ SOPICKI  
ALEKSANDER FILIP ŻARNECKI

Faculty of Physics, University of Warsaw, Poland

WOJCIECH KOTLARSKI

Institut für Kern- und Teilchenphysik, TU Dresden, Germany

*Received 31 December 2021, accepted 10 January 2022,  
published online 28 February 2022*

One of the primary goals of the proposed future collider experiments is to search for dark matter (DM) particles using different experimental approaches. High-energy  $e^+e^-$  colliders offer a unique possibility for the most general search based on the mono-photon signature. As any  $e^+e^-$  scattering process can be accompanied by a hard photon emission from the initial state radiation, an analysis of the energy spectrum and angular distributions of those photons can be used to search for hard processes with invisible final-state production. Processes of DM production via mediator exchange are considered for the International Linear Collider (ILC) and Compact Linear Collider (CLIC) experiments. The detector effects are taken into account within the *Delphes* fast simulation framework. Limits on the light DM production in a simplified model are set as a function of the mediator mass and width based on the expected two-dimensional distributions of the reconstructed mono-photon events. The experimental sensitivity is extracted in terms of the DM production cross section. Limits on the mediator couplings are then presented for a wide range of mediator masses and widths.

DOI:10.5506/APhysPolBSupp.15.2-A10

## 1. Introduction

It is a common belief that the Standard Model (SM) cannot be the ultimate theory of particle physics and a more fundamental description of our

---

\* Presented by A.F. Żarnecki at the XLIV International Conference of Theoretical Physics “Matter to the Deepest”, 15–17 September, 2021.

Universe must exist. It could also manifest itself by “new physics” phenomena, processes extending Beyond the Standard Model (BSM). In particular, there are many hints for the existence of dark matter (DM), and significant experimental effort is being put into different DM detection scenarios. Unfortunately, the nature of DM is unknown and there are very many possible scenarios, resulting in a wide range of masses and couplings to consider.

There are compelling scientific arguments for a new electron–positron collider operating as a “Higgs factory”. Such a collider, producing copious Higgs bosons in a very clean environment, would result in dramatic progress in our understanding of the Higgs boson properties, but also contribute to other precision measurements, including flavour physics and the top-quark physics, and to searches for BSM phenomena. The two linear  $e^+e^-$  collider options, ILC [1] and CLIC [2], offer also the possibility to extend the research domain into the TeV range. This is of particular interest for different BSM searches, and this is why we will focus on these two proposals in the following.

High-energy  $e^+e^-$  machines offer many complementary options for DM searches [3]. Three frontiers can be considered: Higgs precision, high intensity, and energy frontier measurements. Precision measurements in the Higgs sector will be sensitive to many BSM scenarios involving Higgs boson couplings to the new massive states or new Higgs-like scalar mediators. Using the high-energy, high-intensity electron and positron beams, linear colliders will also enable running fixed-target experiments, both beam dump experiments and dedicated experiments using single beams, significantly extending the sensitivity to light DM production scenarios. Direct pair production of DM particles can also be considered at high-energy  $e^+e^-$  colliders. This process can be detected, if additional hard photon radiated from the initial state, see Fig. 1, is observed in the detector. This so-called mono-photon signature is considered the most general approach to search for DM particle production. Presented in this contribution are results concerning the DM pair production with mono-photon signature at future linear  $e^+e^-$  colliders, ILC and CLIC.

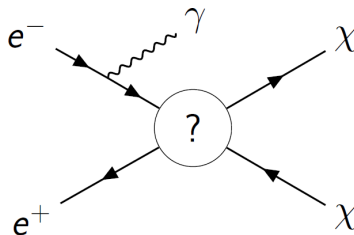


Fig. 1. Diagram describing DM particle pair production process with additional ISR photon radiation.

## 2. Colliders and experiments

The Technical Design Report (TDR) for the International Linear Collider (ILC), based on the technology of superconducting accelerating cavities, was presented in 2013 [4]. The baseline design assumes starting at a centre-of-mass energy of 250 GeV, followed by 500 GeV and 1 TeV considered as the possible upgrade [1]. The schematic layout of the 500 GeV ILC, with a footprint of about 31 km, is shown in Fig. 2. The baseline design includes polarisation for both  $e^-$  and  $e^+$  beams, of 80% and 30%, respectively. Total of  $4000 \text{ fb}^{-1}$  of data is assumed to be collected at 500 GeV stage, with 80% of the integrated luminosity taken with the LR and RL beam polarisation combinations ( $2 \times 1600 \text{ fb}^{-1}$ ), and only 20% with the RR and LL beam polarisation combinations ( $2 \times 400 \text{ fb}^{-1}$ ).

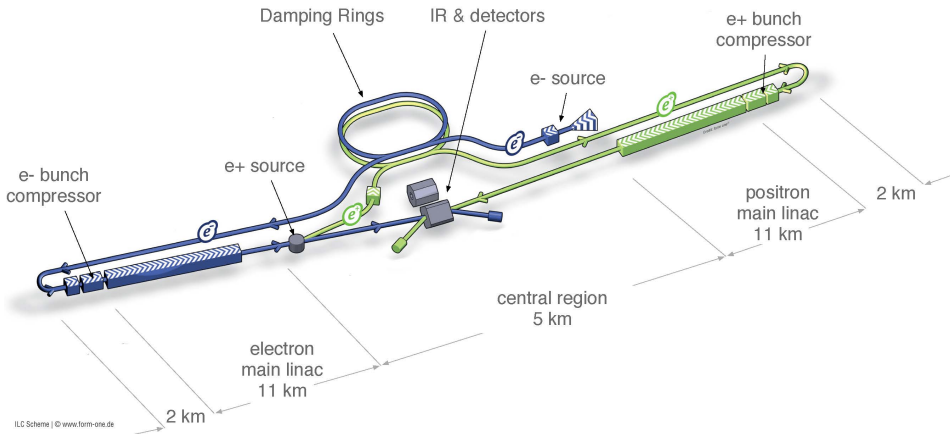


Fig. 2. Schematic layout of the ILC in the 500 GeV configuration.

Conceptual Design (CDR) for Compact Linear Collider (CLIC) at CERN was presented in 2012 and the updated design was presented for the recent European Strategy Update [2]. With the novel two-beam acceleration scheme, an accelerating gradient of up to 100 MV/m can be obtained. This opens the possibility of reaching the collision energy of 3 TeV with a footprint of 50 km, see Fig. 3. Only electron beam polarisation of 80% is included in the CLIC baseline design. At the 3 TeV stage, the total integrated luminosity of  $5000 \text{ fb}^{-1}$  is expected, with 80% ( $4000 \text{ fb}^{-1}$ ) collected with the left-handed electron beam polarisation and 20% ( $1000 \text{ fb}^{-1}$ ) with the right-handed electron beam [5].

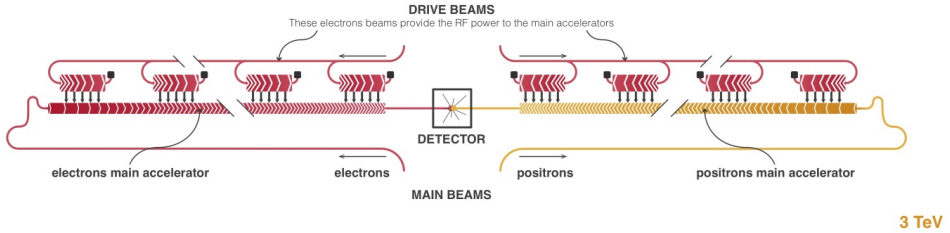


Fig. 3. Schematic layout of the CLIC accelerator for the 3 TeV stage.

Detector designs for ILC and CLIC were based on the same set of requirements. In particular, a single-particle reconstruction and identification is assumed, following the Particle Flow approach [6]. This approach is expected to give the best possible jet energy estimate resulting from combining calorimeter measurements for neutral particles with much more precise track momentum measurements for the charged ones. Simulation studies indicate that a resolution of  $\sigma_{1/p_T} \sim 2 \times 10^{-5} \text{ GeV}^{-1}$  is feasible for high-momentum tracks produced at large angles, resulting in the expected jet energy resolution for high-energy jets of  $\sigma_E/E = 3\text{--}4\%$ . For very good detector hermeticity and efficient suppression of backgrounds to processes with missing energy, instrumentation extending down to a minimum angle of  $\theta_{\min} \sim 5 \text{ mrad}$  is planned. The two detector concepts considered in the presented study, ILD [7, 8] for the ILC and CLICdet [9] for CLIC, are shown in Fig. 4.

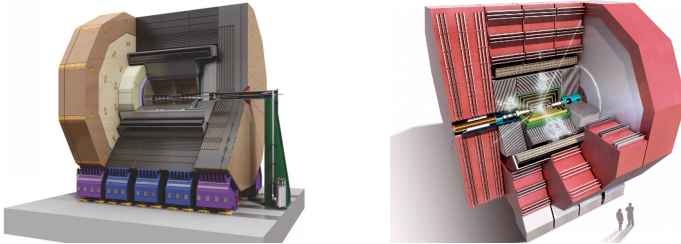


Fig. 4. Detector concepts for the future linear  $e^+e^-$  colliders: ILD for the ILC (left) and CLICdet for CLIC (right).

### 3. Simulating mono-photon events

For a proper estimate of the mono-photon signature sensitivity, a consistent simulation of BSM processes and of the SM backgrounds is crucial. From the experimental point of view, the “irreducible” background to radiative DM pair production comes from radiative neutrino pair production events, see Fig. 5. An additional background contribution, resulting from finite detector acceptance and reconstruction efficiency, is expected from the radiative Bhabha scattering. The Whizard program [10, 11], which is widely

used for  $e^+e^-$  collider studies, provides the ISR structure-function option that includes all orders of soft and soft-collinear photons as well as up to the third order in high-energy collinear photons. However, photons generated by *Whizard* in this approximation cannot be considered as ordinary final-state particles, as they represent all photons radiated in the event from a given lepton line. Also, the ISR structure function cannot properly account for hard non-collinear photon radiation. The proper solution is to generate all “detectable” photons on the Matrix Element (ME) level. This, however, requires a proper procedure for matching soft ISR radiation with hard ME simulation, to avoid double-counting.

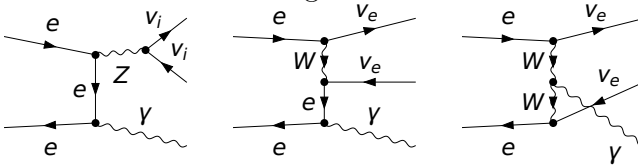


Fig. 5. Diagrams describing the neutrino pair production process with additional photon radiation.

A dedicated procedure for matching ISR and ME regimes was proposed in [12]. It is based on two variables, calculated separately for each emitted photon, used to describe the kinematics of the photon emission

$$q_- = \sqrt{4E_0 E_\gamma} \sin \frac{\theta_\gamma}{2},$$

$$q_+ = \sqrt{4E_0 E_\gamma} \cos \frac{\theta_\gamma}{2},$$

where  $E_0$  is the nominal electron or positron beam energy, while  $E_\gamma$  and  $\theta_\gamma$  are the energy and scattering angle of the emitted photon in question. Detector acceptance in the  $(q_+, q_-)$  plane expected for the future ILC and CLIC experiments is presented in Fig. 6. The red dashed lines indicate the cut used to separate the “soft ISR” emission region (to the left and below the dashed line) from the region described by the ME calculations (to the right and above the dashed line). With this cut, only the photons generated on the ME level can enter the detector acceptance region.

Validity of the proposed matching procedure was verified by comparing results of the *Whizard* simulation with those from the semi-analytical  $\mathcal{K}\mathcal{K}$  MC code [13, 14], for the radiative neutrino pair production events. Results of the comparison are presented in Fig. 7 [12]. After imposing an additional cut on the photon energy and emission angle (corresponding to the expected detector acceptance and reconstruction threshold), distributions of the number of reconstructed photons and the photon transverse momentum agree very well for the two approaches.

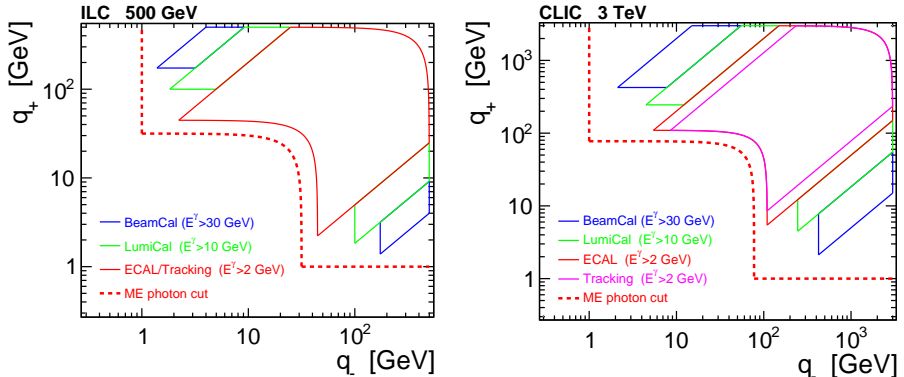


Fig. 6. Detector acceptance in the  $(q_+, q_-)$  plane expected for the future experiments at 500 GeV ILC (left) and 3 TeV CLIC (right). The red dashed lines indicate the cut used to restrict the phase space for ME photon generation [15].

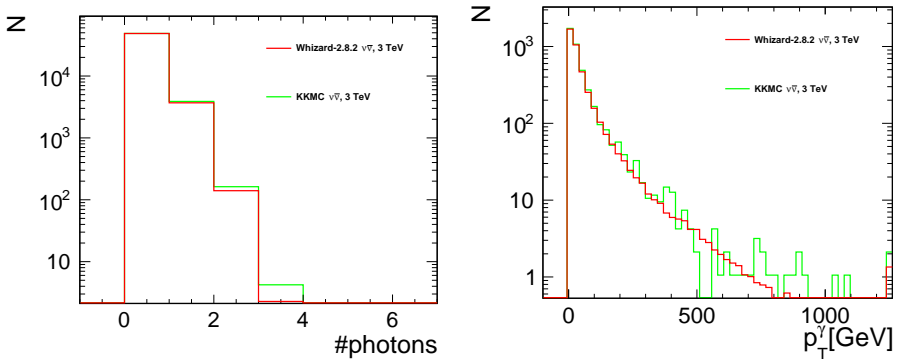


Fig. 7. Distributions of the number of photons (left) and transverse momentum (right) in the neutrino pair production events generated by *Whizard* and the *KKMC*, for collision energy of 3 TeV, after hard photon selection. Distributions are normalised to the number of events expected for an integrated luminosity of  $1 \text{ fb}^{-1}$  [12].

For calculating the DM pair production cross section and generating signal event samples with *Whizard*, the dedicated model [16] was encoded into *FeynRules* [17, 18] and exported in the *UFO* format [19]. Shown in Fig. 8 there is the cross section for DM production,  $e^+e^- \rightarrow \chi\chi$ , as a function of the  $e^+e^-$  collision energy. Pair-production of light Dirac DM,  $m_\chi = 50 \text{ GeV}$ , is considered for a scenario with the vector mediator of 300 GeV and different mediator widths, as indicated in the plot. A possible beam polarisation and beam energy spectra are not taken into account. We consider the mediator mass, width, and coupling to electrons as the independent model parameters, with the total mediator width assumed to

be dominated by decay to the DM particles. In this approximation, cross-section dependence on the DM particle couplings is absorbed in the total mediator width and the results hardly depend on the DM particle type or coupling structure.

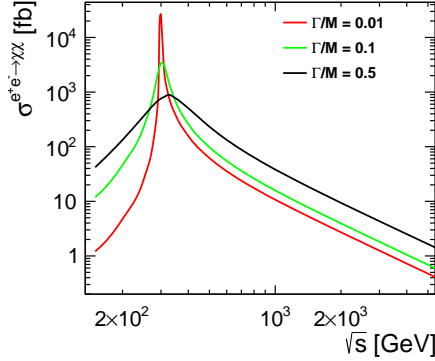


Fig. 8. Cross section for DM production in  $e^+e^-$  collisions as a function of the collision energy  $\sqrt{s}$ . Expectations for pair production of light Dirac DM ( $m_\chi = 50$  GeV) are shown for the scenario with the vector mediator of 300 GeV and different mediator widths. The mediator coupling to electrons is set to 0.01.

In the matching procedure described in [12], events with the ISR photon emitted in the ME phase-space region (refer to Fig. 6) are removed from the analysis (the so-called “ISR rejection”). This can result in up to 50% correction to the DM production cross section, as shown in Fig. 9. It is important to notice that the impact of the ISR rejection procedure is much stronger for light and narrow mediator scenarios ( $M_Y \ll \sqrt{s}$ ,  $\Gamma/M \ll 1$ ) than for the heavy mediator exchange ( $M_Y \gg \sqrt{s}$ ). The impact of the ISR rejection is only reduced for the resonant mediator production,  $M_Y \approx \sqrt{s}$ , when the photon radiation is kinematically suppressed.

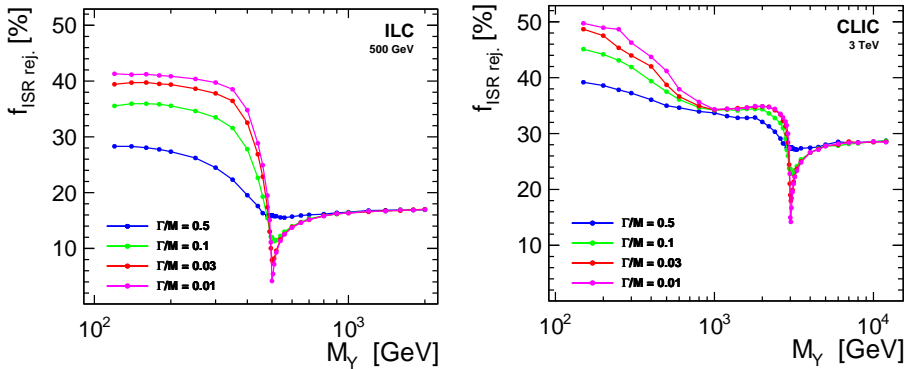


Fig. 9. Fraction of Whizard events, which are removed by the ISR rejection procedure, as described in [12]. See the text for details.

Most of the DM pair production events will remain “invisible” in the detector. While radiation of one or more photons (on ME level) is expected in up to 50% of these events, most of these photons go along the beam-line and escape detection. Only a small fraction of DM pair production events is reconstructed as mono-photon events in the detector. The fraction of “tagged” events also depends significantly on the mediator mass and width, as shown in Fig. 10. Presented results are based on the fast detector simulation framework Delphes [20] in which the two detector models were implemented, including a detailed description of the calorimeter systems in the very forward region.

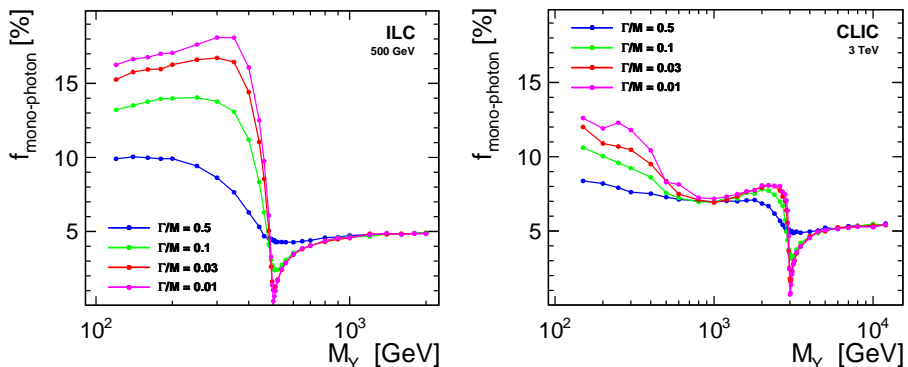


Fig. 10. Fraction of dark matter pair production events, which are reconstructed as mono-photon events in the detector, as a function of the assumed mediator mass, for the ILC running at 500 GeV (left) and CLIC running at 3 TeV (right), and different fractional mediator widths, as indicated in the plot.

#### 4. Mono-photon results

Most of the mono-photon results presented in the past were obtained using the heavy mediator approximation. We will summarise the most recent results from CLIC and ILC before presenting results from the dedicated study, properly taking the finite mediator mass into account.

##### 4.1. Heavy mediator approximation

The potential for detecting DM at the 3 TeV CLIC was investigated in [21]. Detector acceptance, efficiency, and resolution effects were modelled on the generator level. For the mono-photon signature, only events with high-energy, isolated photon, and no other “hard” activity in the detector were considered. Different approaches to detect (or exclude) the DM production signal were considered. The ratio of photon energy distributions measured for the left-handed and right-handed electron beam polarisation



was selected as the distribution most sensitive to the BSM contribution and least sensitive to the systematic effects. The fit to the cross-section ratio distribution also results in the strongest exclusion limits on the radiative DM production cross section, as shown in Fig. 11. Limits on the mono-photon cross section were then translated to the expected exclusion range in the DM-mediator mass space, as shown in Fig. 12 (left) for different mediator

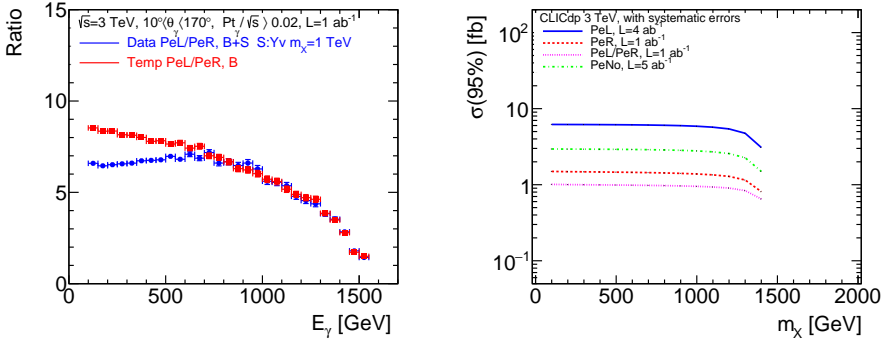


Fig. 11. Results of the mono-photon study for CLIC at 3 TeV [21]. Left: ratio of photon energy distributions measured for the left-handed and right-handed electron beam polarisation, for SM background (red) and after including the DM production contribution with the vector mediator exchange (blue points). Right: exclusion limits on the cross section for DM pair production with the mono-photon signature, for different analysis scenarios.

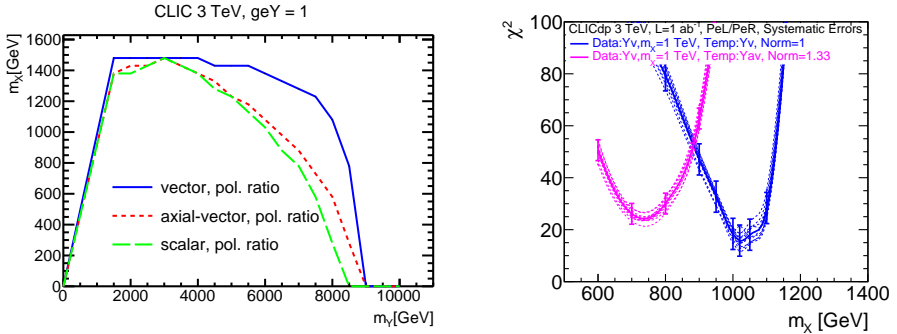


Fig. 12. Results of the mono-photon study for CLIC at 3 TeV [21]. Left: exclusion limits in the DM *versus* the mediator mass plane ( $m_Y$ ,  $m_\chi$ ) for the mediator coupling to electrons,  $g_{eY} = 1$ . Right: expected dependence of the  $\chi^2$  fit values as a function of the assumed dark matter particle mass. Pseudo-data corresponding to the vector mediator mass of 3.5 TeV and the DM mass of 1 TeV are compared with model predictions for the heavy vector (blue) and the axial-vector (purple) mediator exchange.

coupling types. For a light DM particle, the mediator exclusion range extends up to 9 TeV. If significant excess of mono-photon events is observed, the DM mass in a TeV range can be extracted with a 1% accuracy, as indicated by  $\chi^2$  fit results presented in Fig. 12 (right).

A corresponding study based on the full detector simulation has been also performed for the ILD detector at the ILC [22]. Photon energy distribution reconstructed after event selection cuts was used to set limits on the BSM contribution. Distributions expected for the ILC running at 500 GeV for different signal scenarios and SM backgrounds are presented in Fig. 13. After event selection and background suppression cuts, the remaining background is dominated by radiative neutrino pair production events. From comparison

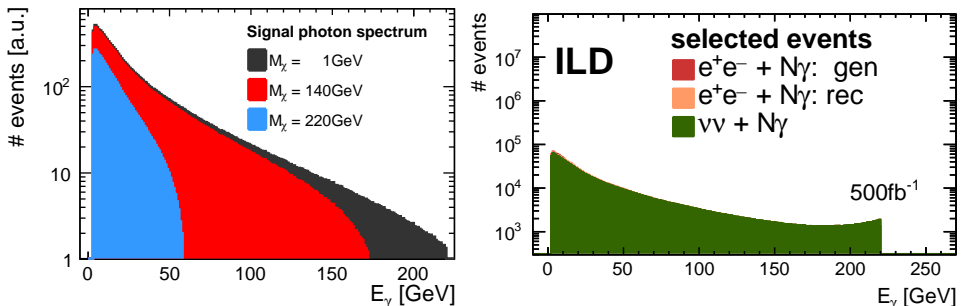


Fig. 13. Results of the full-simulation mono-photon study for the ILD [22]. Photon energy distribution for the ILC running at 500 GeV and  $500 \text{ fb}^{-1}$  of data collected with unpolarised beams, after the event selection cuts. Left: for signal of DM pair production assuming different DM particle masses, as indicated in the plot. Right: for the expected SM background contributions.

of the expected signal and background event distributions, limits on the mediator mass scale are extracted in the heavy mediator limit (operator mass scale in the EFT approach). Expected limits strongly depend on the assumed beam polarisation, as shown in Fig. 14.

By combining runs with different beam polarisation settings, the impact of systematic uncertainties can be significantly reduced. From the combined analysis of all collected data, the expected mass scale limit for the vector mediator scenario extends from 1.4 TeV for ILC running at 250 GeV to about 3 TeV for 500 GeV ILC, assuming that DM particles are light.

Mediator mass scale limits expected from different future colliders, calculated in the EFT approach, are compared in Fig. 15 [23] for the scalar mediator exchange scenario. While these searches, testing mediator couplings to quarks or leptons, are complementary, mass reach of future  $e^+e^-$  machines is comparable to that of hadron colliders, including FCC-hh.

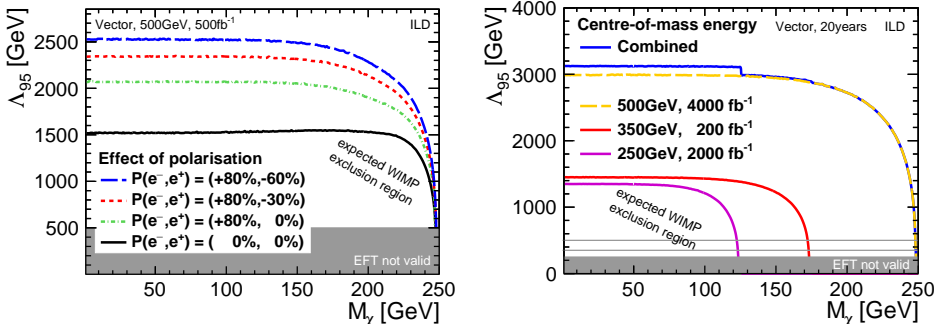


Fig. 14. Results of the full-simulation mono-photon study for the ILD [22]. Expected 95% C.L. limits for the vector operator mass scale, as a function of the assumed DM particle mass. Left: for  $500 \text{ fb}^{-1}$  of data collected at 500 GeV with different beam polarisation combinations. Right: for subsequent stages of the ILC running.

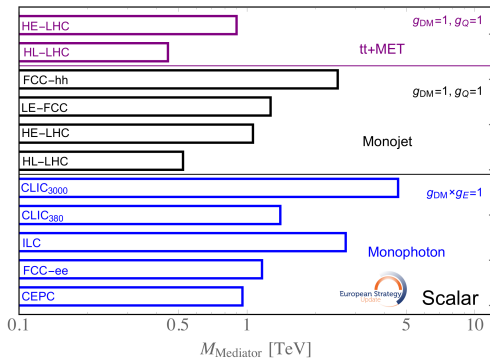


Fig. 15. Summary of  $2\sigma$  sensitivity to scalar mediator mass at future colliders for simplified models with a DM mass of  $M_{\text{DM}} = 1 \text{ GeV}$  and for the couplings shown in the figure [23].

#### 4.2. Light mediator exchange

It is important to notice that DM production via light mediator exchange is still not excluded by the existing experimental data for scenarios with very small mediator couplings to SM. Coupling limits for light mediator scenarios, which were set at LEP and by the LHC experiments, are of the order of 0.01 or above. As mentioned before, pair production of DM particles at the ILC and CLIC was also studied for scenarios with light mediators and small mediator couplings to the SM particles [15]. The study focused on scenarios with very small mediator couplings to SM, when the total mediator width is dominated by invisible decays,  $\Gamma_{\text{SM}} \ll \Gamma_{\text{DM}} \approx \Gamma_{\text{tot}}$ . An “experimental-like” approach is adopted, focused on setting the DM pair production cross-section limits as a function of the mediator mass and width, assuming that

DM particles are light (mass of fermionic DM is fixed to  $m_\chi = 50$  GeV for all results presented in the following). Limits on the production cross section are extracted from the two-dimensional distributions of the reconstructed mono-photon events in pseudorapidity and transverse momentum fraction. Distributions expected at 500 GeV ILC, for SM backgrounds and an example DM production scenario, are compared in Fig. 16. The transverse momentum fraction,  $f_T^\gamma$ , is a logarithm of the transverse momentum scaled to span the range between the minimum and maximum photon transverse momentum allowed for a given rapidity.

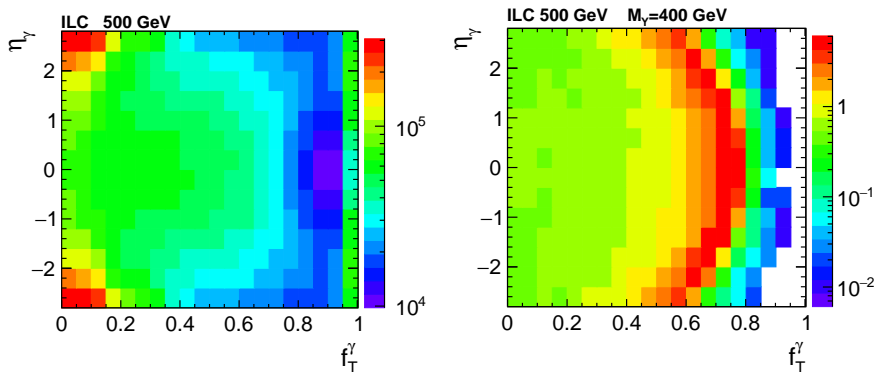


Fig. 16. Pseudorapidity *versus* transverse momentum fraction for mono-photon events at 500 GeV ILC running with  $-80\%/+30\%$  electron/positron beam polarisation and integrated luminosity of  $1.6 \text{ ab}^{-1}$ . Left: for the sum of considered SM backgrounds. Right: for pair production of Dirac fermion DM particles with  $m_\chi = 50$  GeV and vector mediator mass of  $M_\gamma = 400$  GeV, assuming total production cross section of  $1 \text{ fb}$  [15].

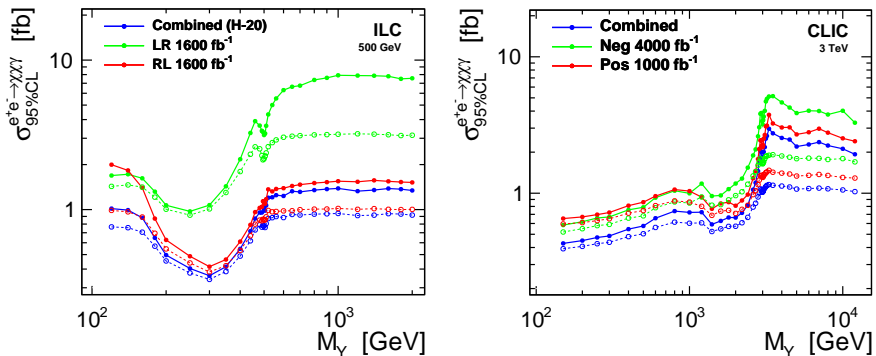


Fig. 17. Limits on the cross section for the radiative light DM pair production processes with vector mediator exchange at 500 GeV ILC (left) and 3 TeV CLIC (right), for mediator width  $\Gamma/M = 0.03$ , with (solid line) and without (dashed line) taking into account systematic uncertainties [15].

Cross-section limits for radiative DM production (for events with tagged photon) at 500 GeV ILC and 3 TeV CLIC, for the vector mediator exchange scenario, are compared in Fig. 17. Combined analysis of data taken with different beam polarisation combinations results in the strongest limits, also reducing the impact of systematic uncertainties. Systematic effects are also suppressed when searching for on-shell production of narrow mediator, *i.e.* for  $M_Y < \sqrt{s}$  (assuming  $\Gamma/M \ll 1$ ).

After correcting for the hard photon tagging probability (refer to Fig. 10), limits for the total DM pair production cross section can be extracted. Presented in Fig. 18 there are limits expected from the combined analysis of data taken with different beam polarisations, for different fractional mediator widths assuming vector mediator exchange and for different mediator couplings.

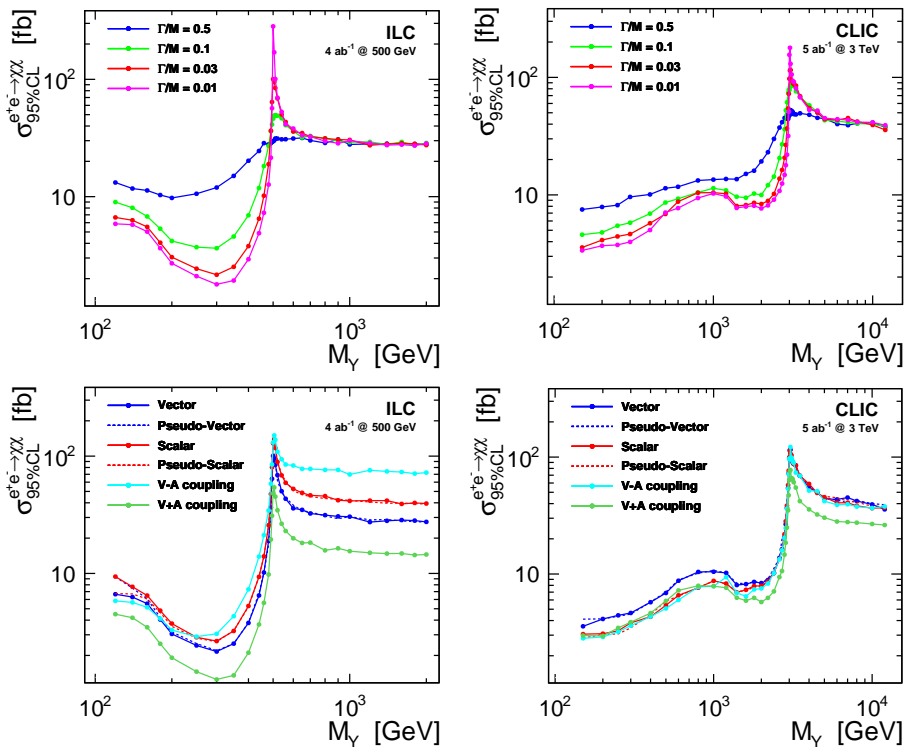


Fig. 18. Limits on the cross section for light fermionic DM pair production processes with  $s$ -channel mediator exchange for the ILC running at 500 GeV (left) and CLIC running at 3 TeV (right). Top row: for vector mediator exchange and different fractional mediator widths. Bottom row: for different mediator coupling scenarios and relative mediator width,  $\Gamma/M = 0.03$ . Combined limits corresponding to the assumed running scenarios are presented with systematic uncertainties taken into account [15].

pling scenarios for narrow mediator exchange,  $\Gamma/M = 0.03$ . The strongest limits are obtained for processes with light mediator exchange and for a narrow mediator widths, whereas for heavy mediator exchange ( $M_Y \gg \sqrt{s}$ ) cross-section limits no longer depend on the mediator width. Limits are significantly weaker for narrow mediator with  $M_Y \approx \sqrt{s}$ , when photon radiation is significantly suppressed. Also compared in Fig. 18 there are combined cross-section limits for different mediator coupling scenarios. It is interesting to note that for processes with light mediator exchange, the model dependence of the total cross-section limits is weaker than for the heavy mediator case. Also, running scenario assumed for CLIC, with 80% of integrated luminosity devoted to running with the negative electron beam polarisation, results in cross-section limits less sensitive to mediator coupling structure than the ILC running scenario assuming equal polarisation sharing.

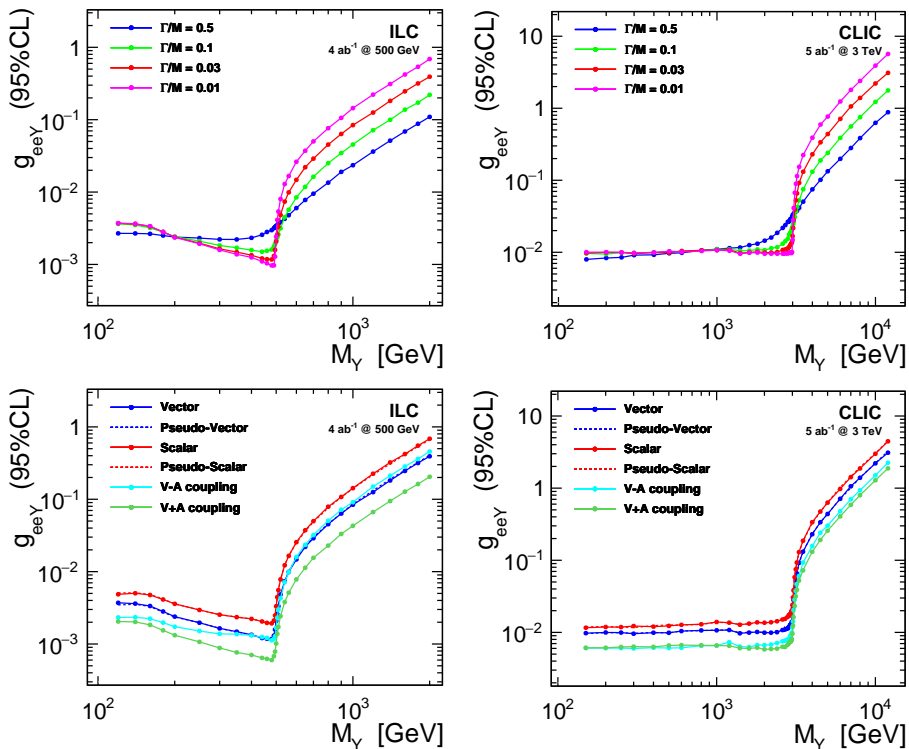


Fig. 19. Limits on the mediator coupling to electrons for the ILC running at 500 GeV (left) and CLIC running at 3 TeV (right). Top row: for vector mediator exchange and different fractional mediator widths. Bottom row: for different mediator coupling scenarios and relative mediator width,  $\Gamma/M = 0.03$ . Combined limits corresponding to the assumed running scenarios are presented with systematic uncertainties taken into account [15].

Shown in Fig. 19 there are expected limits on the mediator coupling to electrons, corresponding to the cross-section limits presented in Fig. 18. For light mediator exchange,  $M_Y < \sqrt{s}$ , the coupling limits hardly depend on the mediator mass and width, showing only moderate dependence on the assumed coupling structure. For the heavy mediator exchange, the coupling limits increase with the mediator mass squared,  $g_{eeY} \sim M_Y^2$ , as expected in the EFT limit.

The cross-section limits obtained for the heavy mediator exchange scenarios can also be translated into the effective mediator mass scale limits in the EFT approach

$$\Lambda^2 = \frac{M_Y^2}{|g_{eeY} g_{\chi\chi Y}|}.$$

Compared in Fig. 20 there are the mediator mass scale limits resulting from the ILD analysis [22] based on the full detector simulation and the EFT approach, and the result from the light mediator exchange analysis [15] for  $M_Y \gg \sqrt{s}$ , based on the fast detector simulation. Very good agreement between full simulation and fast simulation results is observed confirming that the fast detector simulation used in [15] provides a reliable extrapolation of full simulation results to the low mediator mass domain.

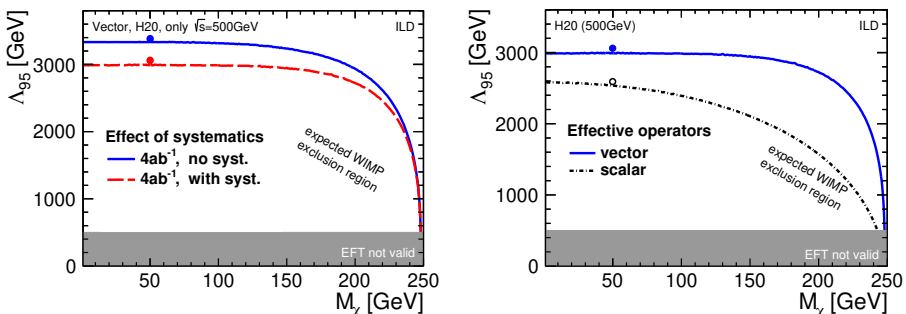


Fig. 20. Expected 95% C.L. limits for the mediator mass scale, as a function of the assumed DM particle mass. Results of the full-simulation mono-photon study in the heavy mediator limit for the ILD [22] (lines) are compared with light mediator analysis [15] (points). Left: impact of systematic uncertainties on the mass scale limits for vector mediator scenario. Right: comparison of limits for scalar and vector mediator hypotheses.

## 5. Conclusions

Future  $e^+e^-$  colliders offer many complementary options for DM searches. Searches based on the mono-photon signature are believed to be the most general and least model-dependent way to look for DM production. A dedicated procedure has been proposed for proper simulation of mono-photon

events in Whizard. In the heavy mediator exchange limit (EFT approach), the sensitivity of future  $e^+e^-$  colliders extends to the mediator mass scales of the order of 10 TeV. A dedicated mono-photon analysis framework was developed for scenarios with light mediator exchange and very small mediator couplings to SM. Future experiments at 500 GeV ILC or 3 TeV CLIC will result in limits on the cross section for the radiative DM pair production,  $e^+e^- \rightarrow \chi\chi\gamma_{\text{tag}}$ , of the order of 1 fb. Corresponding limits on the total DM pair production cross section,  $e^+e^- \rightarrow \chi\chi(\gamma)$ , are of the order of 10 fb (except for the resonance region  $M_Y \sim \sqrt{s}$ ). Limits on the mediator coupling to electrons of the order of  $g_{eeY} \sim 10^{-3}$ – $10^{-2}$  can be set up to the kinematic limit,  $M_Y \leq \sqrt{s}$ . For light mediator scenarios, these limits are more stringent than those expected from direct resonance search in SM decay channels.

We thank members of the CLIC detector and physics (CLICdp) collaboration and the International Large Detector (ILD) concept group for the ILC for fruitful discussions, valuable comments, and suggestions. This contribution was supported by the National Science Centre (NCN), Poland, the OPUS project under contract UMO-2017/25/B/ST2/00496 (2018–2021), the HARMONIA project under contract UMO-2015/18/M/ST2/00518 (2016–2021), and by the German Research Foundation (DFG) under grant number STO 876/4-1 and STO 876/2-2.

## REFERENCES

- [1] P. Bambade *et al.*, «The International Linear Collider: A Global Project», [arXiv:1903.01629 \[hep-ex\]](#).
- [2] A. Robson *et al.*, «The Compact Linear  $e^+e^-$  Collider (CLIC): Accelerator and Detector», [arXiv:1812.07987 \[physics.acc-ph\]](#).
- [3] W. Kotlarski, A.F. Zarnecki, «Probing dark matter with ILC», presented at Particles and Nuclei International Conference — PANIC2021, September 2021, to be published in *Proceedings of Science*.
- [4] C. Adolphsen *et al.* (Eds.), «The International Linear Collider Technical Design Report — Volume 3.II: Accelerator Baseline Design», [arXiv:1306.6328 \[physics.acc-ph\]](#).
- [5] CLICdp, CLIC collaborations, «The Compact Linear Collider (CLIC) — 2018 Summary Report», [arXiv:1812.06018 \[physics.acc-ph\]](#).
- [6] M.A. Thomson, «Particle flow calorimetry and the PandoraPFA algorithm», *Nucl. Instrum. Methods Phys. Res. A* **611**, 25 (2009), [arXiv:0907.3577 \[physics.ins-det\]](#).
- [7] T. Behnke *et al.* (Eds.), «The International Linear Collider Technical Design Report — Volume 4: Detectors», [arXiv:1306.6329 \[physics.ins-det\]](#).



- [8] ILD Collaboration, «International Large Detector: Interim Design Report», [arXiv:2003.01116](#) [[physics.ins-det](#)].
- [9] CLICdp Collaboration, «A detector for CLIC: main parameters and performance», [arXiv:1812.07337](#) [[physics.ins-det](#)].
- [10] M. Moretti, T. Ohl, J. Reuter, «O'Mega: An Optimizing Matrix Element Generator», [arXiv:hep-ph/0102195](#).
- [11] W. Kilian, T. Ohl, J. Reuter, «WHIZARD — simulating multi-particle processes at LHC and ILC», *Eur. Phys. J. C* **71**, 1742 (2011), [arXiv:0708.4233](#) [[hep-ph](#)].
- [12] J. Kalinowski, W. Kotlarski, P. Sopicki, A. Żarnecki, «Simulating hard photon production with WHIZARD», *Eur. Phys. J. C* **80**, 634 (29020), [arXiv:2004.14486](#) [[hep-ph](#)].
- [13] S. Jadach, B.F.L. Ward, Z. Waś, «The Precision Monte Carlo event generator  $\mathcal{KK}$  for two fermion final states in  $e^+e^-$  collisions», *Comput. Phys. Commun.* **130**, 260 (2000), [arXiv:hep-ph/9912214](#).
- [14] S. Jadach, B.F.L. Ward, Z. Waś, «KK MC 4.22: Coherent exclusive exponentiation of electroweak corrections for  $f\bar{f} \rightarrow f'\bar{f}'$  at the LHC and muon colliders», *Phys. Rev. D* **88**, 114022 (2013), [arXiv:1307.4037](#) [[hep-ph](#)].
- [15] J. Kalinowski *et al.*, «Sensitivity of future linear  $e^+e^-$  colliders to processes of dark matter production with light mediator exchange», *Eur. Phys. J. C* **81**, 955 (2021), [arXiv:2107.11194](#) [[hep-ph](#)].
- [16] Model documentation on FeynRules webpage: <https://feynrules.irmp.ucl.ac.be/wiki/SimpDM>
- [17] N.D. Christensen, C. Duhr, «FeynRules — Feynman rules made easy», *Comput. Phys. Commun.* **180**, 1614 (2009), [arXiv:0806.4194](#) [[hep-ph](#)].
- [18] A. Alloul *et al.*, «FeynRules 2.0 — A complete toolbox for tree-level phenomenology», *Comput. Phys. Commun.* **185**, 2250 (2014), [arXiv:1310.1921](#) [[hep-ph](#)].
- [19] C. Degrande *et al.*, «UFO — The Universal FeynRules Output», *Comput. Phys. Commun.* **183**, 1201 (2012), [arXiv:1108.2040](#) [[hep-ph](#)].
- [20] DELPHES 3 Collaboration, «DELPHES 3: a modular framework for fast simulation of a generic collider experiment», *J. High Energy Phys.* **1402**, 057 (2014), [arXiv:1307.6346](#) [[hep-ex](#)].
- [21] CLICdp Collaboration, «Physics performance for Dark Matter searches at  $\sqrt{s} = 3$  TeV at CLIC using mono-photons and polarised beams», [arXiv:2103.06006](#) [[hep-ex](#)].
- [22] M. Habermehl, M. Berggren, J. List, «WIMP dark matter at the International Linear Collider», *Phys. Rev. D* **101**, 075053 (2020), [arXiv:2001.03011](#) [[hep-ex](#)].
- [23] R.K. Ellis *et al.*, «Physics Briefing Book: Input for the European Strategy for Particle Physics Update 2020», [arXiv:1910.11775](#) [[hep-ex](#)].